Cell Metabolism, Volume *29*

Supplemental Information

Metabolic Reprogramming in Astrocytes Distinguishes Region-Specific Neuronal Susceptibility in Huntington Mice

Aris A. Polyzos, Do Yup Lee, Rupsa Datta, Meghan Hauser, Helen Budworth, Amy Holt, Stephanie Mihalik, Pike Goldschmidt, Ken Frankel, Kelly Trego, Michael J. Bennett, Jerry Vockley, Ke Xu, Enrico Gratton, and Cynthia T. McMurray

Table S1. Metabolites Altered in STR *of HdhQ(150/150)* young animals
(Related to Figure 3 and Figure 4)

Lipids				
Metabolite (acyl chain)	**p value**	**Q value**	**(HD/WT)**	**Function**
stearic acid (FFA)(18)	0.025	0.048	1.153	Free Fatty acid (Per)
palmitic acid (FFA)(16)	0.008	0.026	1.256	Free Fatty acid (Per)
lauroyl-carnitine (12)	0.031	0.048	0.672	Mitochondrial import (Per –MT)
myristoyl-carnitine (14)	0.027	0.048	0.627	Mitochondrial import (Per –MT)
Hexadecenoyl-carnitine (16)	0.041	0.051	0.724	Mitochondrial import (Per – MT)
palmitoyl-carnitine (16)	0.009	0.026	0.650	Mitochondrial import (Per – MT)
2-monopalmitin (16)	0.013	0.031	1.483	Palmitic acid β-monoglyceride (MT)
1-monopalmitin (16)	0.015	0.034	1.406	Palmitic acid α-monoglyceride (MT)
1-monostearin (18)	0.030	0.048	1.391	Stearic acid β-monoglyceride (MT)
2-monostearin (18)	0.041	0.051	1.548	Stearic acid α-monoglyceride (MT)
Amino acids, nucleoside, polyamines				
Name	**p value**	**Q value**	**(HD/WT)**	**Function**
Asp	0.011	0.029	0.901	Non-essential aa/glycoprotein synthesis
Trp	0.012	0.030	0.511	Precursor to the neurotransmitter serotonin
homocystine	0.015	0.034	0.520	Breakdown product of protein metabolism
Asn	0.033	0.051	0.488	Nonessential α-amino acid for protein biosynthesis
Met	0.040	0.051	0.740	α-amino acid for protein biosynthesis
Lys	0.041	0.051	0.530	α-amino acid for protein biosynthesis
Thr	0.044	0.051	0.657	Essential amino acid
homoserine	0.046	0.052	0.834	Reactive variant of serine
Tyr*	0.049	0.052	0.512	Production of neurotransmitters
cysteine*	0.049	0.052	0.758	Component of the antioxidant, glutathione
N-acetylaspartate	0.035	0.051	0.477	High in brain, marks viability
methanolphosphate	0.018	0.038	0.813	Derivatives of inosine
FAD	0.008	0.026	1.370	Redox cofactor
spermidine	0.044	0.102	0.409	DNA stability, cell proliferation
Others				
Metabolite	**p value**	**Q value**	**(HD/WT)**	**Function**
ribitol	0.044	0.029	0.608	End product of pentose phosphate pathway
1.5-anhydroglucitol	0.012	0.029	0.813	Associated with glucose fluctuation
inulobiose	0.041	0.051	1.378	1-O-β-D-fructofuranosyl-D-Fructose
glucose	0.044	0.051	0.608	Glycolysis
G1P	0.001	0.016	0.576	Converts to Glucose
G6P	0.026	0.048	0.633	Glycolysis
acetophenone	0.028	0.048	2.634	Aromatic ketone
phosphoric acid	0.048	0.052	1.543	Related with autoimmune disease

* indicates the metabolites that do not pass the additional criteria (FDR<0.056 with Delta=1) by Significance Analysis of Microarray (SAM).

Table S2. TCA intermediates altered in the STR and CBL of *HdhQ(150/150)* animals (related to Figure 3 and Figure 4)

Brain Region	Striatum				Cerebellum			
Age	Young[a]		Old[b]		Young[a]		Old[b]	
	p value	Ratio[c]	p value	Ratio[c]	p value	Ratio[c]	p value	Ratio[c]
malic acid	0.001	0.737	0.496	0.936	0.862	1.012	0.715	0.966
fumaric acid	0.007	0.483	0.531	0.917	0.613	0.954	0.177	0.839
aconitic acid	0.036	0.541	0.628	1.054	0.480	0.946	0.034	0.838
isocitric acid	0.065	0.808	0.397	1.078	0.866	0.989	0.885	1.013
citric acid	0.102	0.849	0.382	1.062	0.566	1.040	0.825	1.023
succinate	0.201	0.865	0.904	1.009	0.069	1.183	0.472	0.915

a. 12-16wks; b. >80wks; c. ratio = HD/WT.

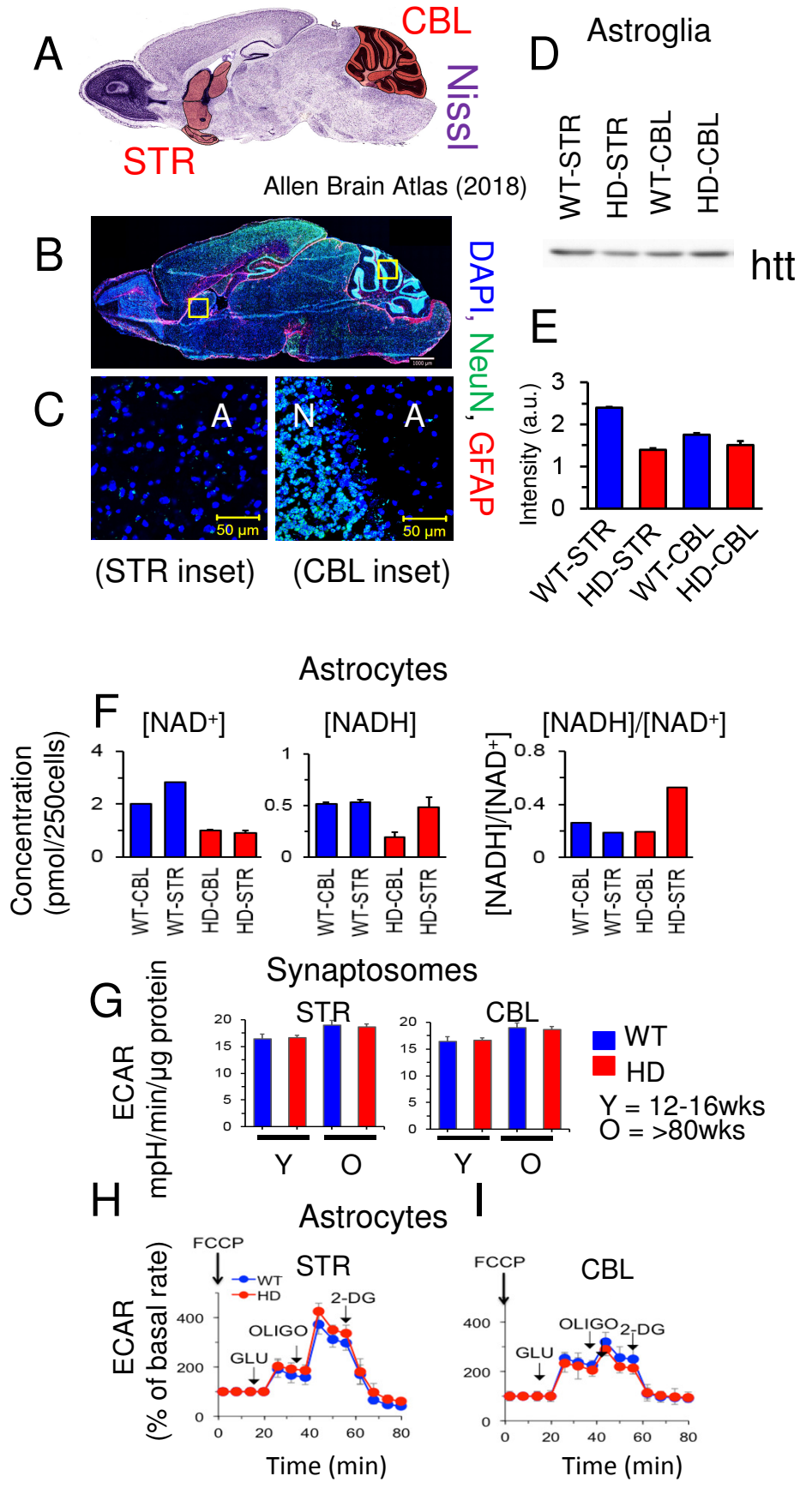
A
CBL
Nissl
STR
Allen Brain Atlas (2018)
B
DAPI, NeuN, GFAP
C
A
N
A
50 µm
50 µm
(STR inset)
(CBL inset)
D
Astroglia
WT-STR
HD-STR
WT-CBL
HD-CBL
htt
E
Intensity (a.u.)
3
2
1
0
WT-STR
HD-STR
WT-CBL
HD-CBL
Astrocytes
F
[NAD+]
[NADH]
[NADH]/[NAD+]
Concentration (pmol/250cells)
4
2
0
1
0.5
0
0.8
0.4
0
WT-CBL
WT-STR
HD-CBL
HD-STR
G
Synaptosomes
ECAR mpH/min/µg protein
STR
CBL
20
15
10
5
0
Y
O
WT
HD
Y = 12-16wks
O = >80wks
H
Astrocytes
I
ECAR (% of basal rate)
FCCP
STR
CBL
WT
HD
2-DG
OLIGO
GLU
400
200
0
0
20
40
60
80
Time (min)

Figure S1

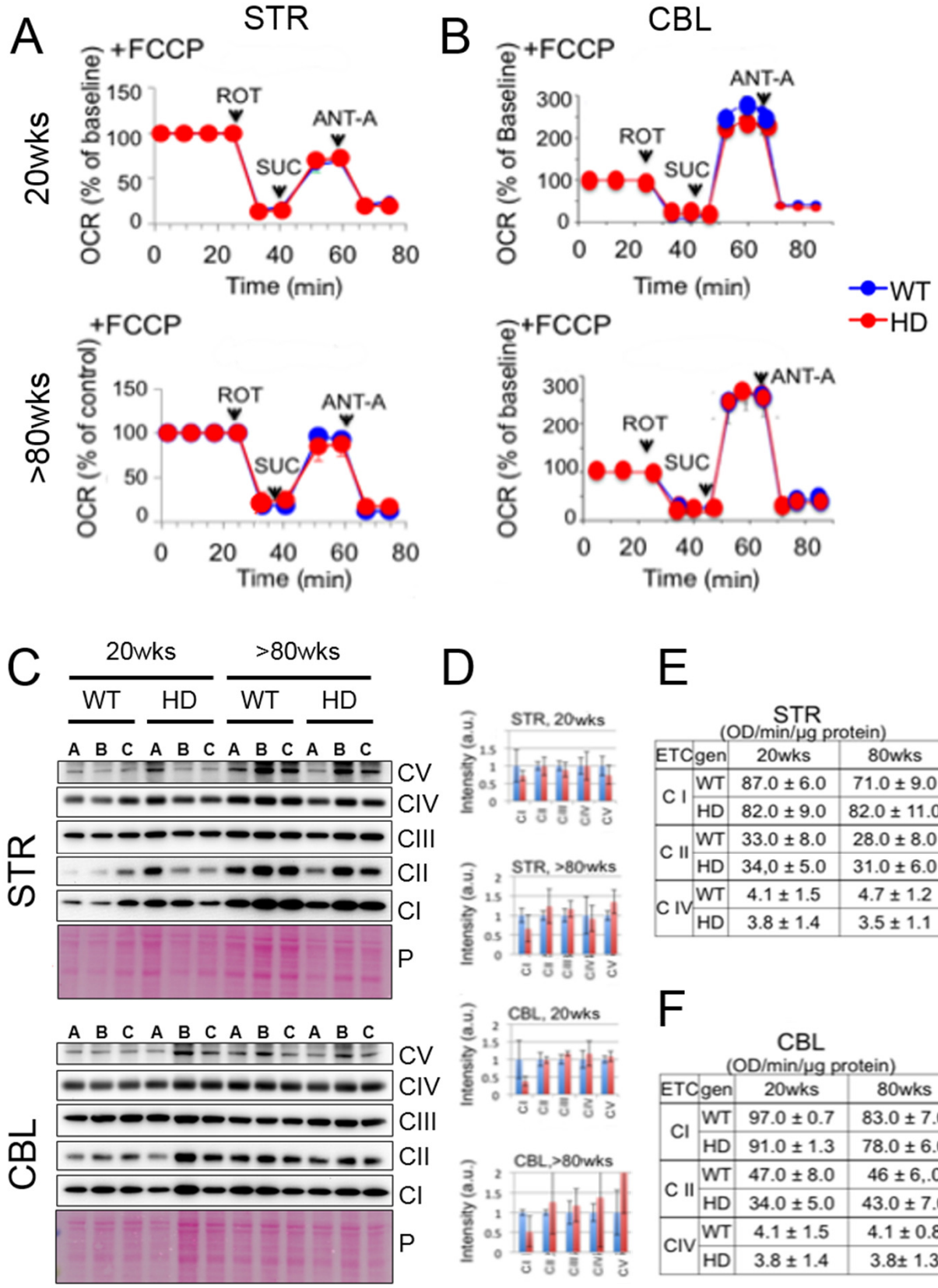

ETC	gen	20wks	80wks
C I	WT	87.0 ± 6.0	71.0 ± 9.0
	HD	82.0 ± 9.0	82.0 ± 11.0
C II	WT	33.0 ± 8.0	28.0 ± 8.0
	HD	34,0 ± 5.0	31.0 ± 6.0
C IV	WT	4.1 ± 1.5	4.7 ± 1.2
	HD	3.8 ± 1.4	3.5 ± 1.1

ETC	gen	20wks	80wks
CI	WT	97.0 ± 0.7	83.0 ± 7.0
	HD	91.0 ± 1.3	78.0 ± 6.0
C II	WT	47.0 ± 8.0	46 ± 6,.0
	HD	34.0 ± 5.0	43.0 ± 7.0
CIV	WT	4.1 ± 1.5	4.1 ± 0.8
	HD	3.8 ± 1.4	3.8± 1.3

Figure S2

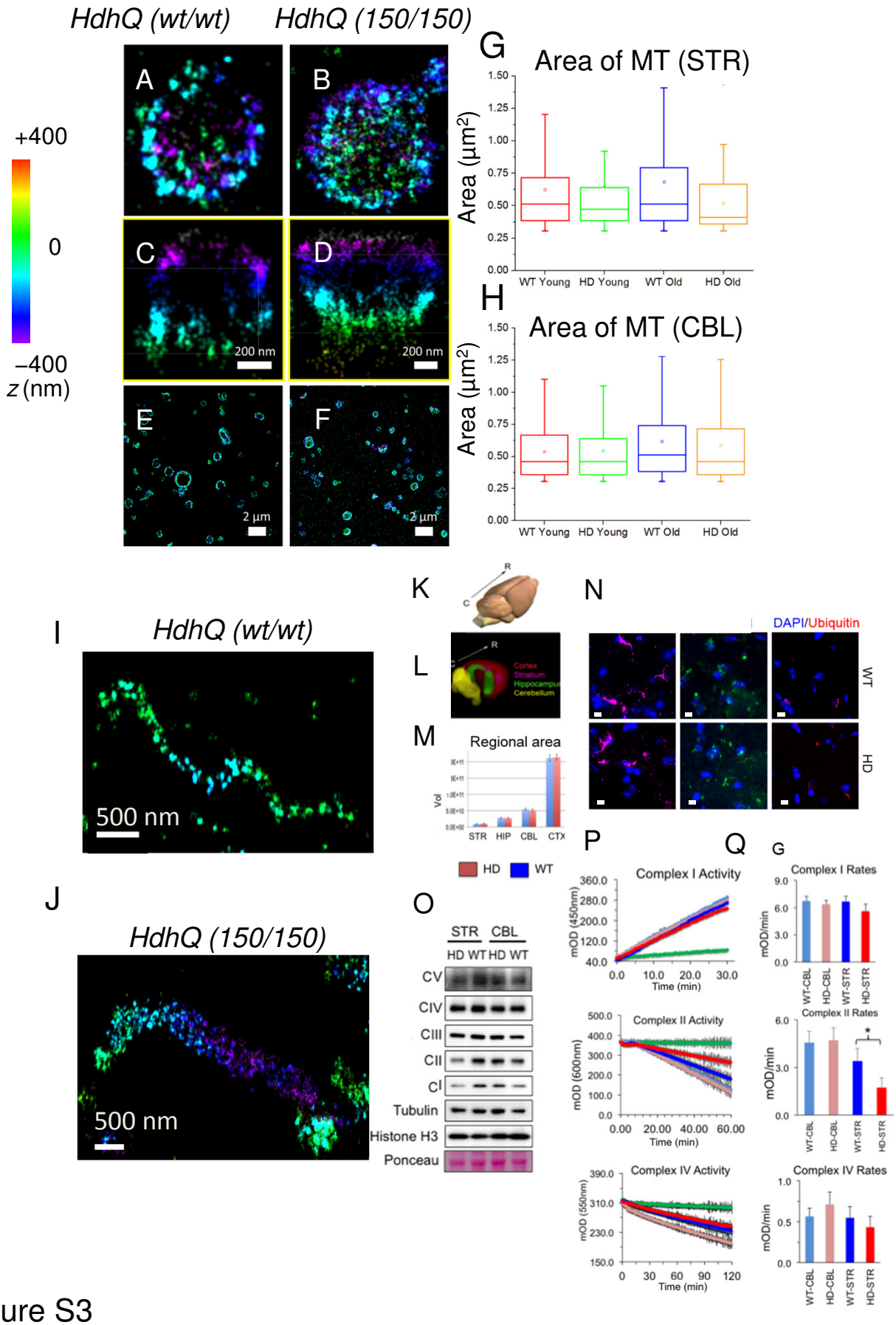
HdhQ (wt/wt)
HdhQ (150/150)
+400
0
–400
z (nm)
A
B
C
D
E
F
200 nm
2 µm
G
Area of MT (STR)
Area (µm²)
WT Young
HD Young
WT Old
HD Old
H
Area of MT (CBL)
I
HdhQ (wt/wt)
500 nm
J
HdhQ (150/150)
K
L
Cortex
Striatum
Hippocampus
Cerebellum
M
Regional area
STR
HIP
CBL
CTX
HD
WT
N
DAPI/Ubiquitin
WT
HD
O
STR
CBL
HD WT HD WT
CV
CIV
CIII
CII
CI
Tubulin
Histone H3
Ponceau
P
Complex I Activity
mOD (450nm)
Time (min)
Complex II Activity
mOD (600nm)
Complex IV Activity
mOD (550nm)
Q
G
Complex I Rates
Complex II Rates
Complex IV Rates
mOD/min
WT-CBL
HD-CBL
WT-STR
HD-STR

Figure S3

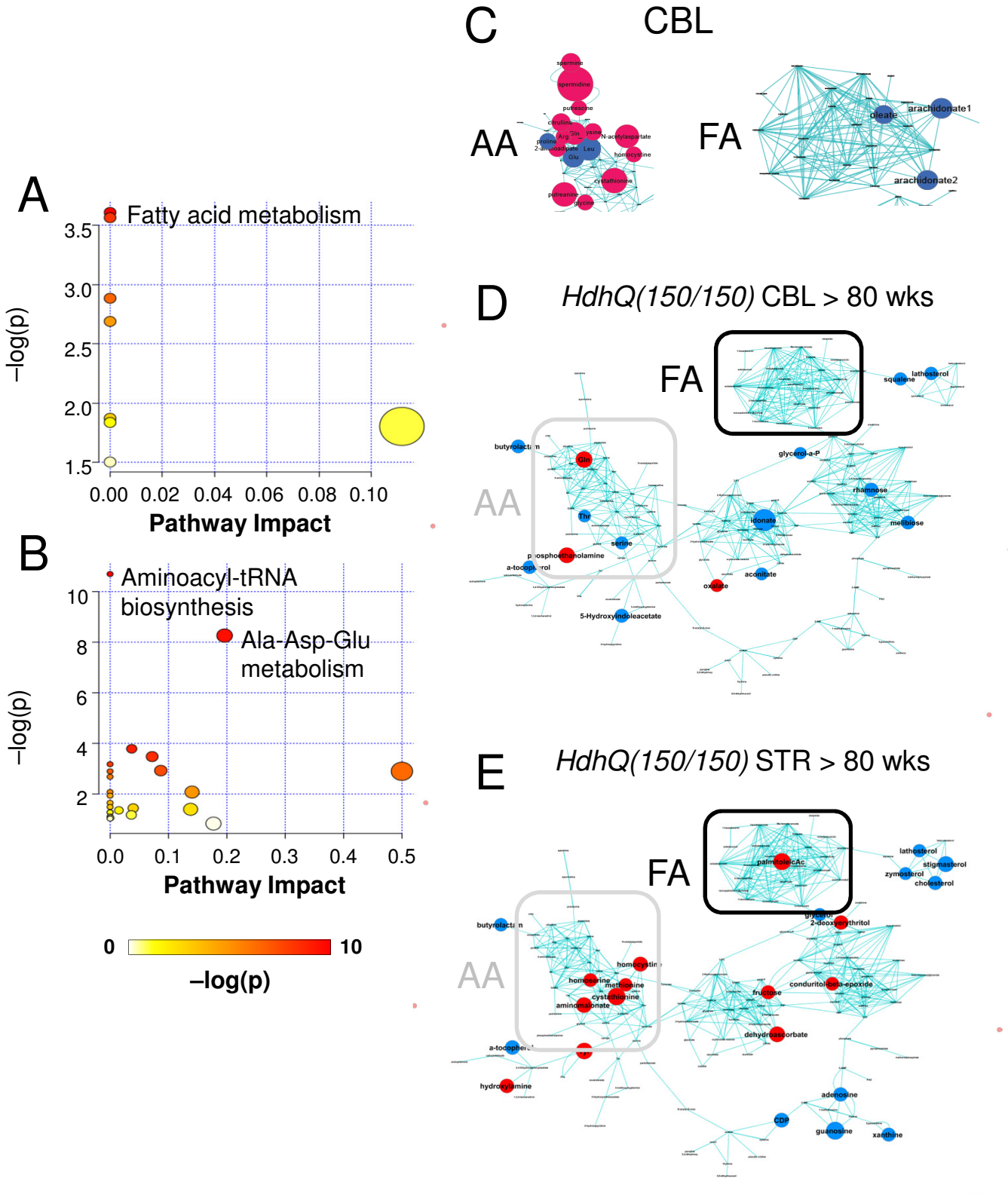
A
Fatty acid metabolism
3.5
3.0
2.5
2.0
1.5
–log(p)
0.00 0.02 0.04 0.06 0.08 0.10
Pathway Impact
B
Aminoacyl-tRNA biosynthesis
Ala-Asp-Glu metabolism
10
8
6
4
2
–log(p)
0.0 0.1 0.2 0.3 0.4 0.5
Pathway Impact
0
10
–log(p)
C
CBL
AA
FA
arachidonate1
oleate
arachidonate2
D
HdhQ(150/150) CBL > 80 wks
FA
AA
squalene
lathosterol
glycerol-a-P
rhamnose
melibiose
idonate
aconitate
oxalate
serine
5-Hydroxyindoleacetate
E
HdhQ(150/150) STR > 80 wks
FA
AA
lathosterol
stigmasterol
zymosterol
cholesterol
palmitoleicAc
homocystin
homoserine
methionine
cystathionine
aminomalonate
fructose
conduritol-beta-epoxide
dehydroascorbate
hydroxylamine
adenosine
CDP
guanosine
xanthine

Figure S4

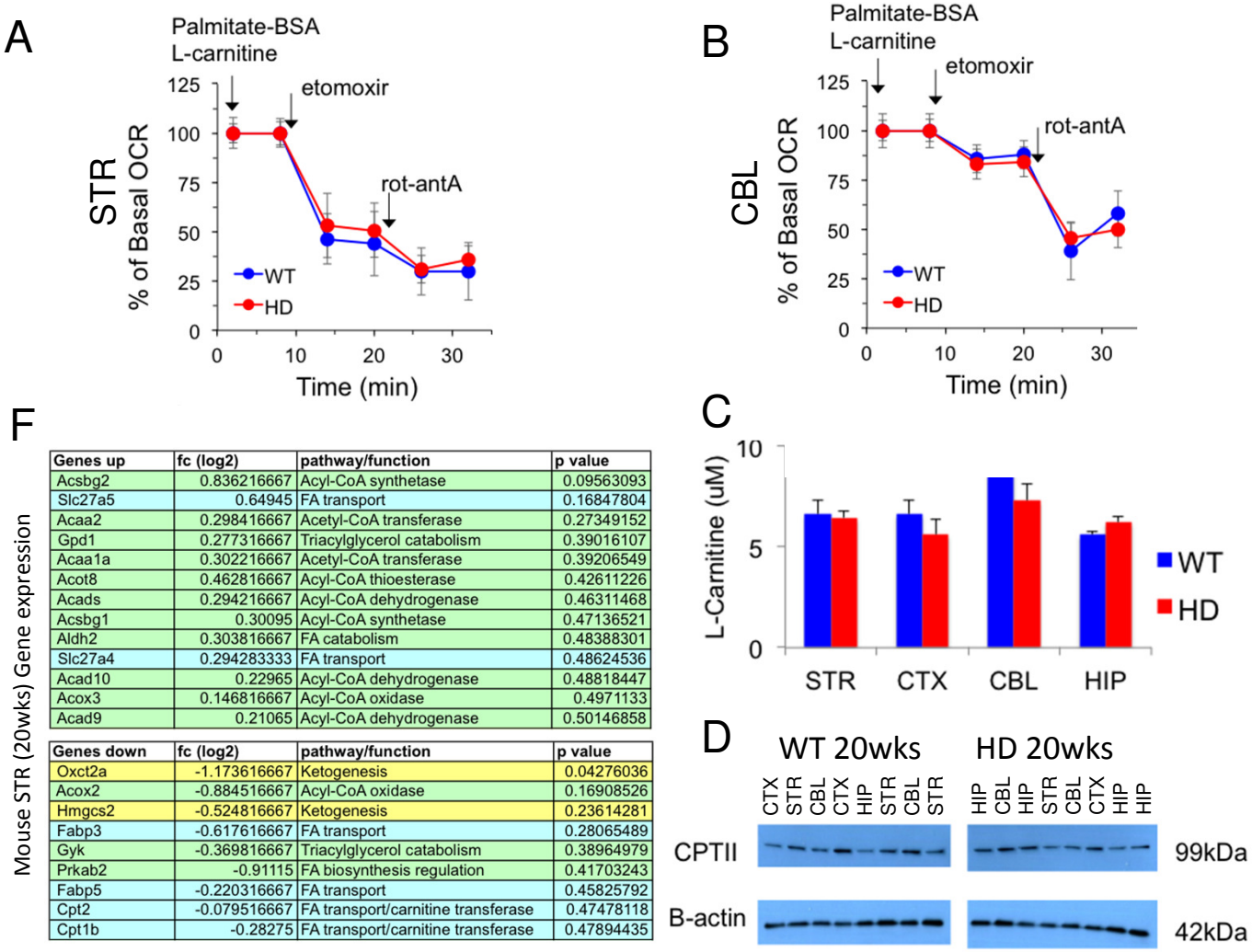

F

Mouse STR (20wks) Gene expression

Genes up	fc (log2)	pathway/function	p value
Acsbg2	0.836216667	Acyl-CoA synthetase	0.09563093
Slc27a5	0.64945	FA transport	0.16847804
Acaa2	0.298416667	Acetyl-CoA transferase	0.27349152
Gpd1	0.277316667	Triacylglycerol catabolism	0.39016107
Acaa1a	0.302216667	Acetyl-CoA transferase	0.39206549
Acot8	0.462816667	Acyl-CoA thioesterase	0.42611226
Acads	0.294216667	Acyl-CoA dehydrogenase	0.46311468
Acsbg1	0.30095	Acyl-CoA synthetase	0.47136521
Aldh2	0.303816667	FA catabolism	0.48388301
Slc27a4	0.294283333	FA transport	0.48624536
Acad10	0.22965	Acyl-CoA dehydrogenase	0.48818447
Acox3	0.146816667	Acyl-CoA oxidase	0.4971133
Acad9	0.21065	Acyl-CoA dehydrogenase	0.50146858

Genes down	fc (log2)	pathway/function	p value
Oxct2a	-1.173616667	Ketogenesis	0.04276036
Acox2	-0.884516667	Acyl-CoA oxidase	0.16908526
Hmgcs2	-0.524816667	Ketogenesis	0.23614281
Fabp3	-0.617616667	FA transport	0.28065489
Gyk	-0.369816667	Triacylglycerol catabolism	0.38964979
Prkab2	-0.91115	FA biosynthesis regulation	0.41703243
Fabp5	-0.220316667	FA transport	0.45825792
Cpt2	-0.079516667	FA transport/carnitine transferase	0.47478118
Cpt1b	-0.28275	FA transport/carnitine transferase	0.47894435

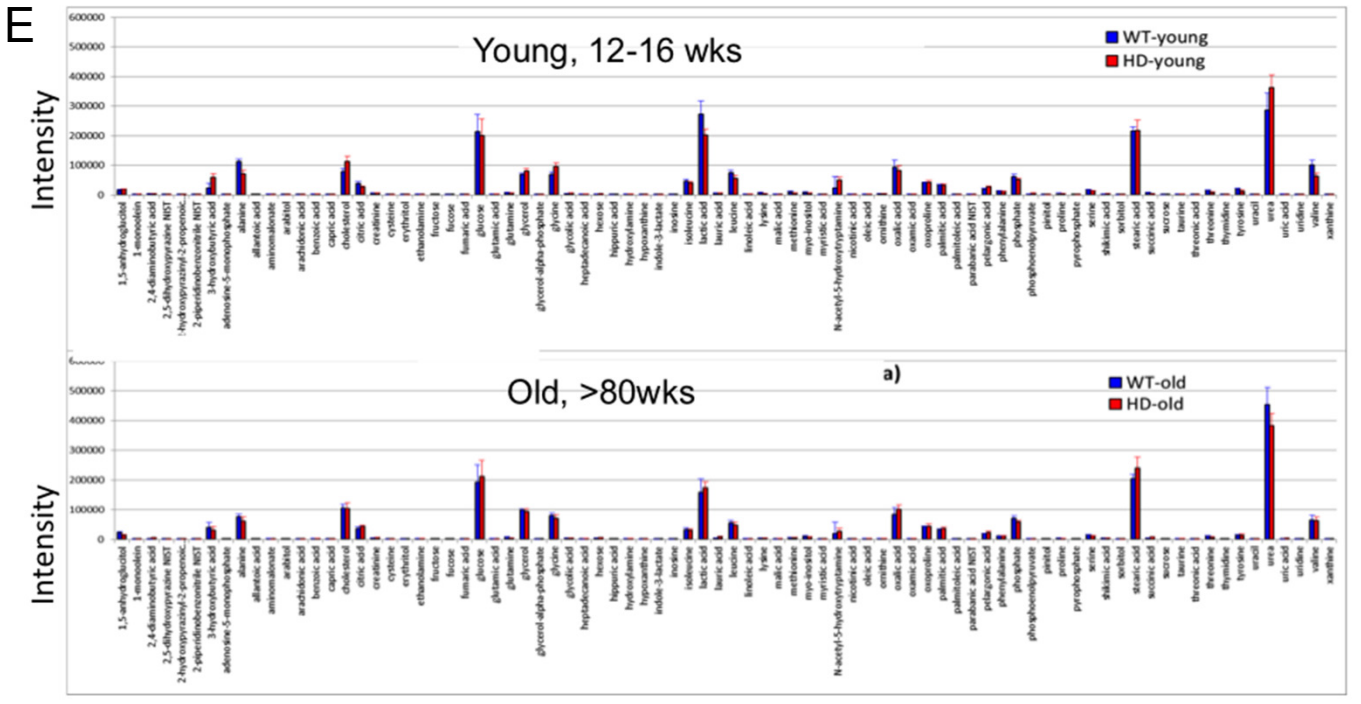

Figure S5

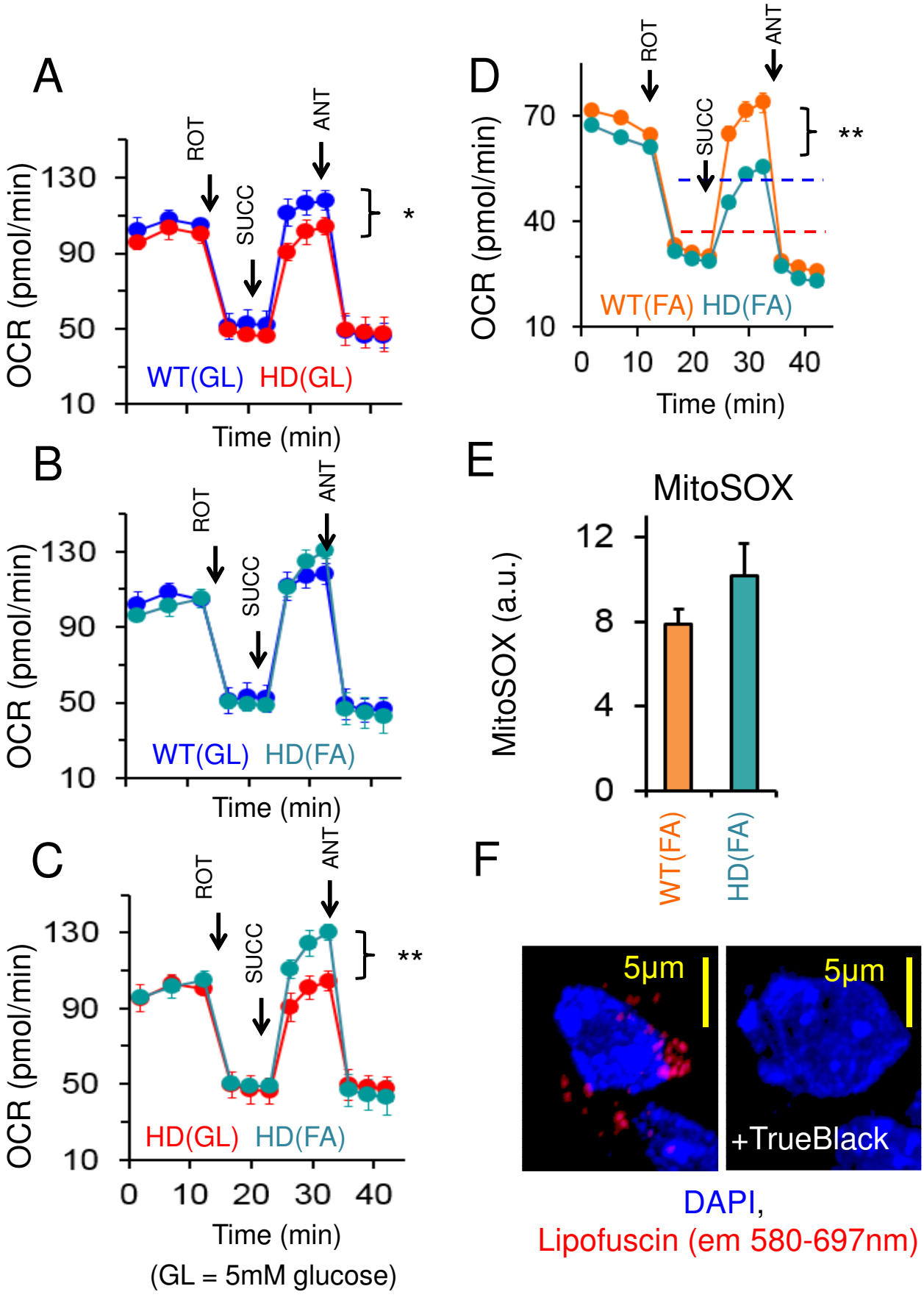
A
ROT
SUCC
ANT
OCR (pmol/min)
130
90
50
10
*
WT(GL) HD(GL)
Time (min)
B
ROT
SUCC
ANT
OCR (pmol/min)
130
90
50
10
WT(GL) HD(FA)
Time (min)
C
ROT
SUCC
ANT
OCR (pmol/min)
130
90
50
10
**
HD(GL) HD(FA)
0 10 20 30 40
Time (min)
(GL = 5mM glucose)
D
ROT
SUCC
ANT
OCR (pmol/min)
70
40
10
**
WT(FA) HD(FA)
0 10 20 30 40
Time (min)
E
MitoSOX
MitoSOX (a.u.)
12
8
4
0
WT(FA)
HD(FA)
F
5µm
5µm
+TrueBlack
DAPI,
Lipofuscin (em 580-697nm)

Figure S6

SUPPLEMENTAL FIGURE LEGENDS

Figure S1. Astrocyte-rich regions in the STR and CBL have similar cell content (Related to Figure 1).

(A) A representative saggital section from an *HdhQ(150/150)* animal used for FLIM scanning. The cartoon (red overlay on Nissl stained tissue) shows the striatum (STR) and cerebellum (CBL), as indicated.

(B) A representative saggital section from an *HdhQ(150/150)* animal stained to visualize astrocytes and neurons. The section was stained with DAPI (blue), which identifies all cell nuclei and the NeuN antibody (green) which stains only neurons. The neuronal cells are distinguished as turquoise by overlap of the green and blue signals, while astrocytes are blue. Astrocyte processes are stained by GFAP (red). Yellow boxes indicate the regions, which are magnified in (C).

(C) Magnified image of the scanned regions boxed in C. (Left, STR) Neurons (N)(turquoise) are interspersed among 80-90% astrocytes (A) (blue). (Right, CBL) A border area in the CBL contains a densely staining neuronal population (N) (turquoise) which lies adjacent to astrocytes (A) (blue). The less dense astrocyte segment is similar in composition to the STR (left).

(D) The level of expressed mhtt in astrocytes isolated from STR and from CBL of *(HdhQ(wt/wt))(WT)* and (*HdhQ(150/150))(HD)* animals. The western blot was probed with anti-htt antibody (Invitrogen MAB 2168). (n = 2).

(E) Quantification of the chemiluminescence from the secondary antibody horseradish peroxidase (HRP) used in the western blots for (D). The bands were normalized for total protein. Astrocytes

from individual animals (n = 3) were pooled in the experiment, and measured in duplicate. Error bars represent SE.

(F) NADH/NAD^+ ratio is elevated in STR relative to the CBL of *HdhQ(150/150)* mice. Colorimetric analysis for NAD^+ and NADH levels from striatal and cerebellar astrocytes from *HdhQ(wt/wt)* (WT) (blue) or *HdhQ(150/150)* mice (red). NADH alone, NAD^+ alone, and the NADH/NAD^+ ratio were determined for n=250 cells using a commercial Abcam(AB65348) kit, measured in duplicate. In all panels, the error bars represent SE.

(G) The activity of the glycoytic enzymes is equivalent in striatal and cerebellar synaptosomes under basal conditions at young (Y) (12-16 weeks) and old (O) (>80 weeks) ages. Glycolysis was measured as the extracellular acidification rate (ECAR) (ΔpH/min/µg of total protein) in the presence of 15mM D-glucose and measured using a Seahorse XF96 Extracellular Flux Analyzer. *HdhQ(wt/wt)* (WT) (blue) and *HdhQ(150/150)(HD)* mice (red). Error bars are SE (n = 3-6 biological replicates, each replicate was measured 8-15 times).

(H and I) The ECAR with time for FCCP-stimulated astrocytes from the (H) STR and the (I) CBL was measured after addition of glucose to glucose-starved synaptosomes. Oxidative phosphorylation was blocked (with oligomycin) leaving only the glycolytic pathway for consumption of glucose. Lastly glycolysis was blocked with the hexokinase inhibitor, 2-deoxyglucose (2-DG). ECAR was measured as a function of time (in minutes) after addition of substrates and inhibitors. There were regional but no genotype-specific differences in ECAR. GLU is glucose, OLIGO is oligomycin (an inhibitor of complex V). The addition of reagents is indicated by the arrows. HD astrocytes (red); WT astrocytes (blue). Each experiment was performed with a minimum of n = 3 astrocyte samples, measured 3-8 times for each sample. n = 30-50 cells. *HdhQ(wt/wt)* (WT) or *HdhQ(150/150)* (HD). Error bars represent SE.

Figure S2. There are no bioenergetic defects in synaptosomes from *HdhQ(150/150)* and *HdhQ(wt/wt)* littermates in any brain region at any age (Related to Figure 2)

(A and B) Bioenergetic plots of OCR expressed versus time (minutes) exrpessed as % of control for astrocytes from STR (A) and CBL (B). The decoupler FCCP was added first to maximize mitochondrial electron flow, and inhibitors were added as indicated by black arrows. ROT is rotenone; SUC is succinate; and ANT-A is antimycin-A. Blue is WT and red is HD.

(C and D) The ETC complexes in synaptosomes from WT and HD animals were equally well expressed as detected by antibodies to the resolved proteins on SDS-PAGE gels (C). The protein expression levels in young (20wk) and old (>80wks) animals (C) were quantified (D) from the antibody staining intensities for CI (21kDa, ndufb8 subunit), CII (30kDa, SDH subunit B), CIII (49.5kDa, uqcrc2), CIV (40kDa, oxidative phosphorylation subunit 1) and CV (55kDa, ATP synth subunit alpha antibodies), normalized for Ponceau staining intensity (red-pink gels). (n = 2), error bars represent SE.

(E and F) Quantified enzymatic activity of ETC complexes CI, CIII, and CIV in synaptosomes from (E) STR and (F) CBL of WT and HD animals at young (20wk) and old (>80wks) ages, The enzymatic activities of CI, CIII, and CIV were measured as absorbance versus time (minutes) per µg protein. Activity was equivalent in synaptosomes of young (12-16weeks) or old (>80weeks) animals of both genotypes. (n = 3). CI activity measured at 450nm, CII activity measured at 600nm, CIV activity measured 550nm. Error bars represent SE.

Figure S3. Structure and function are not altered in brain synaptosomes, while CII activity is reduced in astrocytes (Related to Fig. 2).

(A and B) Zoomed-in representative 3-D image of an intact synaptosome from *HdhQ(wt/wt)* (WT) (A) and *HdhQ(150/150)* (HD) (B) animals (top panel). Scale bar is 200nm. The pseudocolor scale is shown (left).

(C and D) z cross-section of the top row images (A and B), respectively. Scale bar is 200nm. The pseudocolor scale is shown (left).

(E and F) Zoomed-out view displaying a super-resolution image of MT from isolated striatal synaptosomes of *HdhQ(wt/wt)* (WT) (left) and *HdhQ(150/150)* (HD) (right) animals stained with translocase of outer membrane protein 20 (TOM20), Scale bar is 2μm. The pseudocolor scale is shown (left).

(G and H) Box-and-whisker plot of the size distribution of mitochondria in isolated striatal (G) and cerebellar (H) synaptosomes. (top) The imaged samples from left to right: STR of young WT (red) and young HD (green) mice; STR of old WT (blue) and old HD (orange) mice. (H) Same as G for CBL. Size of the MT was determined based on epifluorescence images of TOM20. Note: only structures with size greater than 11 pixels were considered for this analysis; structures below this size are believed to be too small to be mitochondria. The average mitochondrial sizes in the striatal synaptosomes were somewhat smaller than in the CBL of old *HdhQ(150/150)* mice. *P* is two-tailed Student's t-test.

(I and J) 3-D STORM analysis of actin-spectrin cytoskeleton in isolated synaptosomes from *HdhQ(wt/wt)* (I) and *HdhQ(150/150)* (J) littermates. The quality of the synaptosomes preparations was determined in part by the maintenance of cytoskeleton, which is characterized by a stable spacing of spectrin and actin and is documented to be 180-190 nm in axons (Xu et al., 2013). The spectrin spacing in synaptic axons attached to isolated (I) *HdhQ(wt/wt)* brain synaptosomes is

distributed around 100-190 nm, while (J) the spectrin spacing in synaptic axons attached to isolated *HdhQ(150/150)* synaptosomes ranged from 150-180 nm. Scale bar is 500nm. These values are consistent with good structural integrity of the synaptosomes.

(K and L) Representative MRI **f**or a young *HdhQ(wt/wt)* (WT) littermates. As judged by MRI imaging (K), the brain volume was well-developed in the brain of 20 week WT and HD animals. Caudal (C) - rostral (R) orientation of the brain of a 20 week WT animal is indicated. **(L)** Colors delineate the volumes of the CTX (red), STR (purple), HIP (green), and CBL (yellow) (L). Diagnostic imaging performed at the veterinary medicine teaching hospital (VMTH) at University of California Davis. Dimensions of the fields were set to 256x256x100 pixels and the voxel size to 117x117x122μm.

(M) Quantified volumes of brain regions from *HdhQ(wt/wt)* (WT) and *HdhQ(150/150)(HD)* littermates. Blue is WT and red is HD. Error bars represent SE, (n = 3 animals).

(N) Representative immunofluorescent staining of 10μm fixed tissue slices of striatum from brains of young (12-16wks old) *HdhQ(wt/wt)* and *HdhQ(150/150)* animals stained with antibodies against ubiquitin (red), IBA1 (green) and GFAP (magenta) overlaid on stained nuclei (blue, DAPI). These stains are measures of aggregates, activated microglia, and astrocytes respectively. There were no notable abnormalities that are genotype dependent. There was no evidence for microgliosis in the striatum (IBA1), for loss of astrocytes, or for increased aggregates due to disease at 12-16 weeks. Scale bars = 10μm. (Also reported previously in Polyzos *et al.,* 2016).

(O) SDS-PAGE gel images of resolved ETC complexes from astrocytes of STR and CBL of post-natal day (P2) used in the rate analysis (related to Figure 2D). Loading controls are tubulin,

histone H3 and ponceau stain (pink). Gel quantifications are described in Figure 2E and 2F. WT are *HdhQ(wt/wt)* and HD are *HdhQ(150/150)* animals.

(P) Representative kinetic curves to assess the rates of ETC enzyme activity (related to Figure 2D). Data were the results of a colorimetric microplate assay from Abcam (following manufacturers protocols). Plotted is the change in absorbance versus time (minutes) for background, and astrocyte extracts from STR and CBL of WT and HD astrocytes, as indicated: CI activity measured at 450nm, CII activity measured at 600nm, CIV activity measured 550nm. Absorbance versus time plots are matched by color-coding: no sample (green), WT-CBL (light blue), HD-CBL (pink), WT-STR (dark blue), and HD-STR (red). WT are *HdhQ(wt/wt)* and HD are *HdhQ(150/150)* animals.

(Q) The rate (mOD/min) of complex activity is calculated by the slope of kinetic curves in P (related to Figure 2D). The activity of CII is lower in the STR of HD versus WT animals, * is $p = 0.01$ (two-tailed Student's t-test). n = 6 measurements for each astrocyte culture (n = 2). WT are *HdhQ(wt/wt)* and HD are *HdhQ(150/150)* animals.

Figure S4. Metabolic analysis from mass spectrometry (Related to Figure 3 and Figure 4).

(A and B) Pathway over-representation analysis of significantly increased fatty acid metabolites (A) and decreased metabolites, as indicated (B) in HD STR at 12-16 weeks (n = 6). The –log(p) indicates a significant level of pathway alteration cumulatively computed by the significance of metabolite changes in a pathway. Pathway impact represents the readout from pathway topology analysis, based on relative-betweeness centrality. The node size and color are scaled according to statistical significance and pathway impact score, respectively. The color scale is shown.

(C) Enlarged views of MetaMapp panels for FA and AA basal composition in CBL of *HdhQ(wt/wt)* animal (Taken from *Lee et al., 2013*), which is similar to the metabolic composition of the CBL in the disease state.

(D and E) MetaMapp of CBL (D) and STR (E) at 80 weeks (n = 6) for the amino acids (AA) and fatty acid (FA) clusters. Node colors indicate significant changes of metabolite levels ($p < 0.05$, two-tailed Student's t-test) in *HdhQ(150/150) (*HD) brain regions compared to those in *HdhQ(wt/wt)* (WT) (red = elevated metabolites, blue = decreased metabolites in HD brain). Node size represents the fold change of differentially-expressed metabolite in HD brain compared to WT.

Figure S5. The increase in FA metabolites is not due to alterations in FA access, gene expression, or a mitochondrial import block (Related to Figure 4 and Figure 5).

(A, and B) There is no FA import inhibition in MT in STR of *HdhQ(150/150)* relative to *HdhQ(wt/wt)* littermates. The OCR was measured in astrocytes of the STR (A) or the CBL (B) grown in the presence of FAs (0.22mM palmitate-BSA). Import of L-malate and L-carnitine was subsequently measured by the reduction in OCR after addition of etomoxir (an inhibitor of carnitine palmitoyltransferase-1 (CPT-I)). Etomoxir addition reduced the OCR in MT of striatal or cerebellar astrocytes from *HdhQ(150/150)* and *HdhQ(wt/wt)* littermates to the same extent. OCR was further reduced by addition of rotenone (rot) and Antimycin-A (antA), which inhibit the electron transport chain complexes CI and CIV. There was no genotype-dependence to the inhibition. Red is HD and blue is WT.

(C) The L-carnitine levels were similar in both genotypes. Carnitine was measured using a commercial kit (Abcam ab83392). The error bars represent SE.

(D) The level of CPT-II was similar in both genotypes, indicating that the impact of blocking CPT-I was not altered by differences in CII. Antibody staining analysis of CPT-II by SDS-PAGE (WT 20 weeks (left), and HD 20 weeks (right)) was equivalent in astrocytes from *HdhQ(150/150),* with β-actin as a loading control. (n = 3-4 mice brain regions analyzed per sample).

(E) Mass spectrometry analysis of plasma metabolites from 12-16wk or >80wk *HdhQ(150/150)* and *HdhQ(wt/wt)* littermates (n = 6 animals for each group). No significant differences of free FAs are observed from the blood plasma of HD animals relative to WT. Both genotypes show similar levels of other major metabolites including glucose, lactic acid and TCA intermediates. N = 3 pooled samples. Error bars are SE.

(F) Real time PCR analysis for a panel of 80 genes comprising enzymes of FA anabolism, transport, and catabolism. Eighty FA processing genes were assessed for their levels in STR of 20wk animals (3 animals per genotype) by real-time PCR. Some tended to increase and some to decrease, but none were statistically different (two-tailed Student's t-test, $p>0.05$) in striatal brain tissue of HD versus WT animals (where the FA accumulation was evident in their brains) (a partial list of the most significant is shown). Functionality of each gene is grouped as indicated by the color code. Green indicates genes for catabolic enzymes, yellow indicates genes for ketogenic enzymes, and turquoise indicates enzymes for import and transport. Gene expression was not significantly altered in *HdhQ(150/150)* animals at this early age. *P* from two-tailed Student's t-test.

Figure S6. FA addition restores the succinate response in MT of striatal astrocytes in physiological glucose concentrations (5mM) (Related to Figure 6).

(A-C) is simiar to Figure 6A-6C except that GL is 5mM glucose (GL). ROT is rotenone; SUCC is succinate; and ANT is antimycin-A.

(A) Comparison of *HdhQ(wt/wt)* (WT) astrocytes and *HdhQ(150/150)* (HD) astrocytes in GL buffer (p<0.05, two-tailed Student's t-test), (n = 3).

(B) Comparison of *HdhQ(wt/wt)* (WT) astrocytes in GL buffer and *HdhQ(150/150)* (HD) astrocytes in FA buffer (p<0.43, two-tailed Student's t-test), (n = 3).

(C) Comparison of *HdhQ(150/150)* (HD) astrocytes in GL and FA buffer (p<0.005, two-tailed Student's t-test), (n = 3).

(D) Comparison of *HdhQ(wt/wt)* (WT) and *HdhQ(150/150)* (HD) astrocytyes in FA media. FA increased CII-dependent OCR in astrocytes of *HdhQ(wt/wt)* (WT) animals if glucoase was low (p<0.005, two-tailed Student's t-test). Bioenergetic plots of OCR of WT and HD STR astrocytes in FA media, expressed as pmole/min. The decoupler FCCP was added first to maximize mitochondrial electron flow, and inhibitors were added as indicated by black arrows. ROT is rotenone; SUCC is succinate; and ANT is antimycin-A. For comparison red and blue dashed lines are OCR of WT-STR and HD-STR in GL respectively. The assay was performed in n = 3-6 biological replicates with 5-8 repetitions for each cell type.

(E) MitoSOX staining intensity for *HdhQ(150/150)* (HD) or *HdhQ(wt/wt)* (WT) astrocytes at the indicated condiitons. p=0.154, two-tailed Student's t-test. Orange is WT and Turquoise is HD. The assay was performed in n = 3-6 biological replicates with 5-8 repetitions for each cell type.

(F) Perinuclear lipofuscin granules are identified by autofluorescence (Related to Fig. 7). Autofluorescent granules were visualized at 580-697nm in astrocytes in a perinuclear orientation (red, left) after excitation at 561nm (z-stack image). Lipofuscin granule size was $2.09 \pm 0.08\ \mu m^2$

(WT) and 2.93 $\pm$ 0.08 μm^2 (HD) at 100weeks. The signal disappears (right panel) after treatment of the cells with TrueBlack® (a modified form of Sudan Black) known to quench lipofuscin fluorescence. Scale bar is 5μm.